Monthly Notices
of the
ROYAL ASTRONOMICAL SOCIETY

Mon. Not. R. Astron. Soc. **402,** 705–712 (2010) doi:10.1111/j.1365-2966.2009.15538.x

Can X-ray emission powered by a spinning-down magnetar explain some gamma-ray burst light-curve features?

N. Lyons,[1⋆] P. T. O'Brien,[1] B. Zhang,[2] R. Willingale,[1] E. Troja[1,3,4] and R. L. C. Starling[1]

[1]*Department of Physics and Astronomy, University of Leicester, University Road, Leicester LE1 7RH*
[2]*Department of Physics and Astronomy, University of Nevada Las Vegas, 4505 Maryland Parkway, Box 454002, Las Vegas, NV 89154-4002, USA*
[3]*INAF – Istituto di Astrofisica Spaziale e Fisica Cosmica, Sezione di Palermo, via Ugo la Malfa 153, 90146 Palermo, Italy*
[4]*Dipartimento di Scienze Fisiche ed Astronomiche, Sezione di Astronomia, Università di Palermo, Piazza del Parlamento 1, 90134 Palermo, Italy*

Accepted 2009 August 12. Received 2009 August 12; in original form 2009 January 7

ABSTRACT

Long-duration gamma-ray bursts (GRBs) are thought to be produced by the core-collapse of a rapidly rotating massive star. This event generates a highly relativistic jet and prompt gamma-ray and X-ray emission arises from internal shocks in the jet or magnetized outflows. If the stellar core does not immediately collapse to a black hole, it may form an unstable, highly magnetized millisecond pulsar or magnetar. As it spins down, the magnetar would inject energy into the jet causing a distinctive bump in the GRB light curve where the emission becomes fairly constant followed by a steep decay when the magnetar collapses. We assume that the collapse of a massive star to a magnetar can launch the initial jet. By automatically fitting the X-ray light curves of all GRBs observed by the *Swift* satellite, we identified a subset of bursts which have a feature in their light curves which we call an internal plateau – unusually constant emission followed by a steep decay – which may be powered by a magnetar. We use the duration and luminosity of this internal plateau to place limits on the magnetar spin period and magnetic field strength, and find that they are consistent with the most extreme predicted values for magnetars.

Key words: stars: neutron – gamma-rays: bursts.

1 INTRODUCTION

Gamma-ray bursts (GRBs) are thought to be caused by a violent event such as the collapse of a massive star (for long-duration bursts) or the coalescence of two compact objects (for short-duration bursts). These progenitors result in the immediate formation of a black hole which powers a relativistic jet pointing in the direction of the observer. In the standard fireball model, variability in the Lorentz factor of the outflow causes internal shocks which produce the prompt flash of X-ray and gamma-ray emission (Rees & Mészáros 1994; Sari & Piran 1997). When the relativistic outflow sweeps up a sufficient amount of external material, the ejecta is decelerated causing a forward shock which is primarily responsible for the multiwavelength afterglow emission (Katz 1994; Mészáros & Rees 1997; Sari, Piran & Narayan 1998).

Alternatively there is a model that suggests a black hole may not be formed immediately, but instead that a transitory highly magnetized rapidly rotating pulsar, or magnetar, may form (Usov 1992; Thompson 1994), before the star collapses to a black hole (Rosswog & Ramirez-Ruiz 2003). Protomagnetars have very high magnetic field strengths of 10^{16} G (Duncan & Thompson 1992; Duncan 1998) which are thought to be a consequence of millisecond rotation at birth in a core-collapse supernova. Values up to $\sim 10^{17}$ G are implied by observations (Stella et al. 2005). Such objects are considered as a possible central engine for GRBs due to their large rotational energy reservoir, $E_{\rm rot}$. Also, they can be associated with supernovae, as are long GRBs, and their winds are thought to become relativistic like a GRB jet.

Zhang & Mészáros (2001) investigated the observational signature of a spinning-down magnetar as the GRB central engine. Adopting an approximate magnetic dipole radiation model, they infer that the spin-down power of the protomagnetar could produce a period of prolonged constant luminosity followed by a t^{-2} decay. They considered the modification of the forward shock dynamics by magnetar spin-down and predicted a distinct achromatic feature. A similar model was discussed earlier by Dai & Lu (1998) who considered the energy injection to the forward shock by a millisecond pulsar with much a weaker magnetic field. This model is one of the candidates to interpret the majority of the X-ray plateaus observed in many *Swift* GRB afterglows (Nousek et al. 2006; Zhang et al. 2006). This model does not invoke the internal dissipation of the magnetar wind. On the other hand, if the magnetar wind indeed dissipates internally before hitting the blastwave, it is possible that it

⋆E-mail: nal14@star.le.ac.uk

would generate an 'internal' X-ray plateau whose X-ray luminosity tracks the spin-down luminosity if the energy dissipation and radiation efficiency remain constant. If the magnetar undergoes direct collapse into a black hole before spin-down, then the X-ray plateau would be followed by a very steep decay. This is the light-curve feature we investigate, and hereafter we call this feature an 'internal plateau'.

In the *Swift* era, the early X-ray light curve, observed within the first few hours of the GRB, has been found to be complex (e.g. Nousek et al. 2006; O'Brien et al. 2006). The so-called canonical X-ray light curve observed in a significant fraction of GRBs (Evans et al. 2009) has a short period of fast decay, often with flares superimposed, which are usually over within the first hour after the burst. This is followed by a shallower decay period lasting from a few hours up to a day with a temporal decay index $\alpha \sim 0.5$ (where the X-ray flux $f_\nu \propto \nu^{-\beta} t^{-\alpha}$ and β is the spectral index). After this X-ray plateau, there is a smooth transition to a modest power-law decay of $\alpha \sim 1$–1.5.

Willingale et al. (2007) found that the X-ray light curve of most GRBs, including those of the canonical form, can be represented by two components – the prompt and afterglow – plus flares (Section 2). However, we find that in a small minority of bursts a period of relatively constant emission (compared to the general light curve) followed by a steep decline can be identified which does not fit this phenomenological model. The observed feature instead resembles the proposed signature of a magnetar spin-down. Troja et al. (2007) found that such a feature dominates the X-ray light curve of GRB 070110 from ≈1000–20 000 s in and proposed it was due to a spinning-down millisecond pulsar. Starling et al. (2008) found a similar, earlier feature in GRB 070616 ending at about 600 s. Liang, Zhang & Zhang (2007) systematically analysed a sample of X-ray plateaus and identified several more plateaus that are followed by decays with slopes steeper than $\alpha = -3$. It is the combination of a plateau followed by a steep decay which distinguishes these from the canonical behaviour. We regard these objects as candidate internal plateaus.

We have conducted a systematic investigation of the GRB X-ray light curves observed by *Swift* up to the end of 2008. Using an automated fitting procedure in this paper, we identify 10 bursts which may have an emission component powered by magnetar spin-down dominating the light curve for some period of time in the form of an internal plateau. Assuming this internal plateau is caused by the spinning down of a magnetar, we use its properties to constrain the magnetic field and initial spin period of the magnetar. The criteria for selecting those GRBs with internal plateaus are discussed in Section 2. Section 3 compares the properties of the internal plateaus with the magnetar model, and we discuss the implications in Section 4.

2 THE FUNCTIONAL FORM OF *SWIFT* LIGHT CURVES

Over 90 per cent of GRB X-ray light curves are well described by a two-component model with a prompt and an afterglow component as described in Willingale et al. (2007). These components are described by an exponential that relaxes into a power law; this function can be expressed for the prompt component as shown in equation (1). Large flares were masked out of the fitting procedure. Although apparently bright, such flares account for only about 10 per cent of the total fluence in most cases. The prompt emission rises with the time constant t_p and later the emission transitions from an exponential to a power law at point (T_p, F_p), where the subscript 'p' refers to the prompt component of the emission (Willingale et al. 2007). The exponential and power-law decay are both controlled by the index α_p.

$$f_\mathrm{p}(t) = F_\mathrm{p} \exp\left(\alpha_\mathrm{p} - \frac{t\alpha_\mathrm{p}}{T_\mathrm{p}}\right) \exp\left(\frac{-t_\mathrm{p}}{t}\right), \quad t < T_\mathrm{p}$$
$$f_\mathrm{p}(t) = F_\mathrm{p} \left(\frac{t}{T_\mathrm{p}}\right)^{-\alpha_\mathrm{p}} \exp\left(\frac{-t_\mathrm{p}}{t}\right), \qquad t \geq T_\mathrm{p}. \tag{1}$$

For this investigation, we are interested in those GRBs whose early X-ray emission could not be adequately fitted by the Willingale model. Thus, we fitted all the *Swift* GRBs with the model and then examined all cases where the model fails.

The X-ray light curves were derived from the BAT and XRT data using the methods described in O'Brien et al. (2006) and Willingale et al. (2007). BAT and XRT light curves were derived for each GRB using NASA's HEASARC software. The BAT data were extracted over the 15–150 keV band and the BAT spectra were produced using the task BATBINEVT. An estimate of the fractional systematic error in each BAT spectral channel from the BAT calibration data base was added to the spectra using the BATPHASYSERR command. The corresponding response matrices were generated by the command batdrmgen. XRT data were extracted over the 0.3–10 keV band. The light curves were corrected for point spread function losses and exposure variations. The XRT spectra were extracted using the XSELECT software, and the spectra were grouped to have at least 20 counts per channel. The relevant ancillary response files were generated using the task XRTMKARF. Ultraviolet and Optical Telescope (UVOT) data were extracted using the task UVOTEVTLC. The V, B, U and white magnitudes were corrected for Galactic extinction along the line of sight and then converted to monochromatic fluxes at the central wavelength of each filter. The effective mid-wavelength was taken to be 4450 Å for the white filter.

In Fig. 1, we show an example of a GRB that the Willingale model fits well (GRB 060427) and one which it does not (GRB 060510B) and instead demonstrates an internal plateau where the flux remains constant with small fluctuations for about 360 s. It has been suggested that instead of a plateau there is a group of flares very close together, however maintaining a high level of flux for hundreds of seconds with the peak of each flare having almost identical flux seems unlikely. Some of the GRBs for which the model fails were those where a pre-cursor triggered the *Swift* BAT instrument or where very large flares were not fitted. We examined all of the fitted light curves to remove such cases. To be included in the internal plateau sample, a GRB must have the following.

(i) A light curve that could not be adequately fitted by the Willingale model.

(ii) A significant period of time during which the X-ray flux is relatively constant, i.e. at least a third of a decade long.

(iii) A convincing steep decline following the internal plateau which falls by a factor of 10 where $\alpha \geq 4$, so that the emission is likely caused by central engine activity and is not the canonical X-ray plateau.

This gives 10 GRBs with light-curve internal plateau features that resemble the spin-down magnetar model discussed in Zhang & Mészáros (2001).

3 GRBs WITH AN INTERNAL PLATEAU

The 10 GRBs which form our internal plateau sample and values of interest such as the redshift and plateau luminosity are listed in

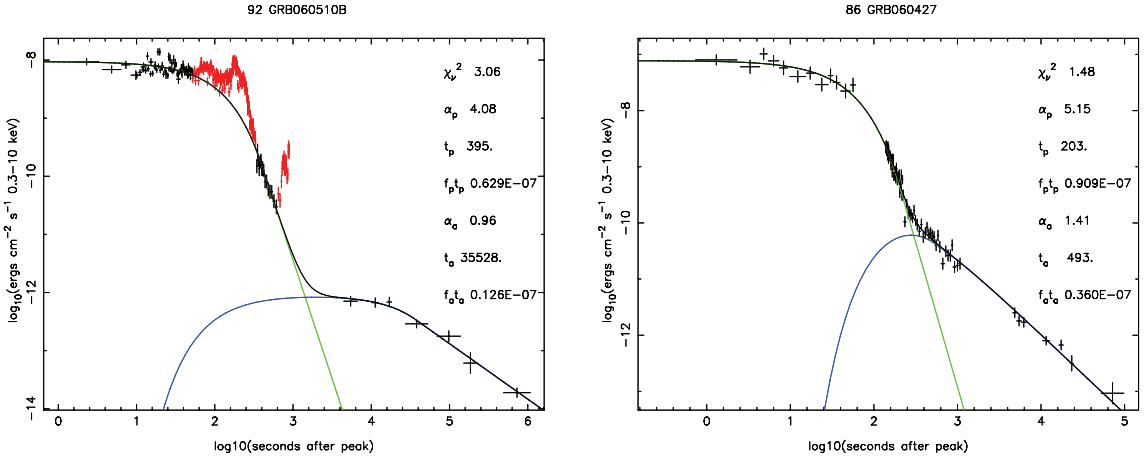

(a) (b)

Figure 1. The left-hand panel shows the light curve in the BAT and XRT for GRB 060510B, and the right-hand panel displays a more typical burst; GRB 060427. The green line represents emission from the burst (prompt) and the blue line emission from the afterglow, as given by the Willingale et al. (2007) model. The portions in red in the left-hand panel are the data (flares and internal plateaus) which the model does not fit.

Table 1. The observed properties of the GRBs with an internal plateau.

GRB	Redshift	Flux[1] (10^{-9} erg cm^{-2} s^{-1}) (0.3–10 keV)	Luminosity[1] (erg s^{-1})	End time[1] (s)	Steep decay
080310	2.426	5.39	2.6e+50	401.9	$11.21^{+1.00}_{-0.50}$
071021	5.0	2.45	6.6e+50	248.3	$9.18^{+1.01}_{-0.474}$
070721B	3.626	0.24	3.0e+49	802.9	$10.31^{+1.42}_{-2.696}$
070616	2.22*	11.44	4.4e+50	585.6	$5.07^{+0.13}_{-0.17}$
070129	2.22*	2.24	8.6e+49	683.0	$7.71^{+0.88}_{-0.67}$
070110	2.352	0.02	8.8e+47	21 887.1	$6.98^{+0.10}_{-0.34}$
060607A	3.082	0.15	1.3e+49	13 294.7	$3.43^{+0.80}_{-0.91}$
060510B	4.9	6.58	1.7e+51	362.9	$10.43^{+0.66}_{-0.58}$
060202	2.22*	2.69	1.0e+50	766.0	$5.70^{+0.17}_{-0.16}$
050904	6.29	1.53	7.1e+50	488.8	$9.364^{+0.91}_{-1.49}$

*Where no measurement is available the redshift is assumed to be the mean of *Swift* GRBs taken from the web site maintained by P. Jakobsson (http://raunvis.hi.is/∼pja/GRBsample.html).
[1]These are parameters related to the plateau, i.e. the end time is the time the plateau ends before the steep decline begins.

Table 1. For the GRBs with an observed redshift in Table 1, the mean redshift is 3.96, significantly higher than the *Swift* mean redshift of 2.22 for all GRBs with measured redshift. A Kolmogorov–Smirnov test with a confidence level of 90 per cent could not prove that the distribution of these redshifts is inconsistent with the *Swift* redshift distribution for all GRBs with measured redshift. The GRBs which display an internal plateau are shown in Fig. 2 and are discussed briefly below.

GRB 080310 has emission that could be an internal plateau followed by a steep decline, which seems to rise above the underlying emission. Also, shortly after the internal plateau there is a flare which peaks at the same flux as the internal plateau. While in this GRB the proposed internal plateau could be due to a multiple number of flares (O'Brien et al., in preparation), we include it in our sample.

GRB 071021 has a possible internal plateau dominating the early X-ray light curve. This is the shortest proposed internal plateau in the sample lasting about 105 s.

GRB 070721B has a possible internal plateau that dominates early in the light curve. Flaring dominates over the internal plateau emission, during the middle of this time interval. This could signify a brief period of accretion on to the protomagnetar. Ignoring the single flare, the emission is similar to that for other internal plateau candidates, so it has been included in the sample.

GRB 070616 is intriguing, in that the emission rises relatively slowly over 100 s to a peak, then persists at a fairly constant level before showing a very rapid decline.

GRB 070129 is similar to GRB 070721B, in that it has a possible internal plateau that is interrupted by a flare followed by a steep decline.

GRB 070110 displays a canonical early light curve with an initial steep decline, but then exhibits a period of relatively constant emission. Following this plateau, the decay is surprisingly steep ($\alpha \sim 7$) decay (Troja et al. 2007). Thus, in this case the protomagnetar survived for much longer than in most of the other GRBs.

GRB 060607A appears to follow the canonical light curve with a 'normal' X-ray plateau with multiple flares preventing a good fit

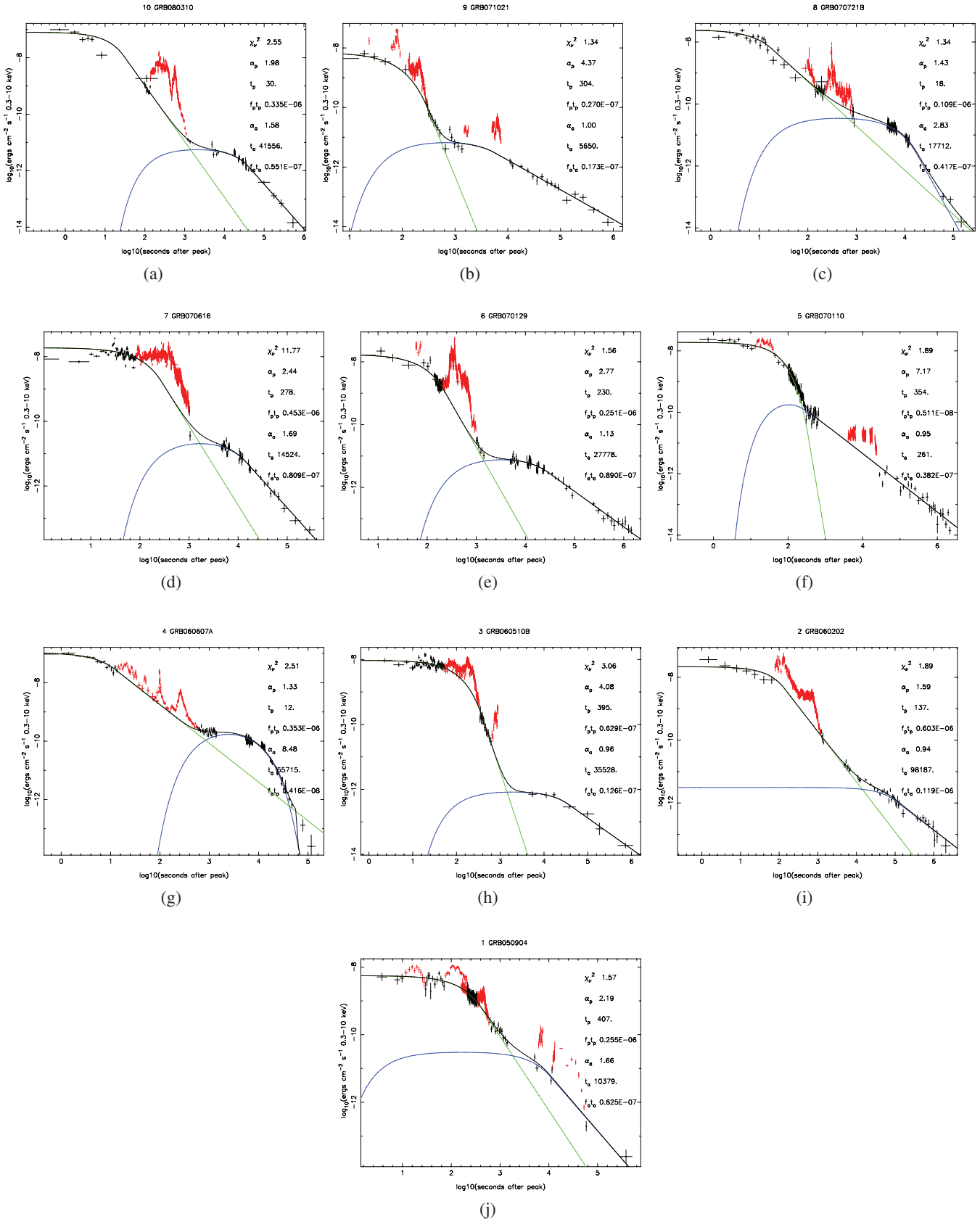

Figure 2. The GRB light curves displaying internal plateau behaviour. The green line represents emission from the burst (prompt) and the blue line emission from the afterglow, as given by the Willingale et al. (2007) model. The portions in red are the data (flares and internal plateaus) which the model does not fit.

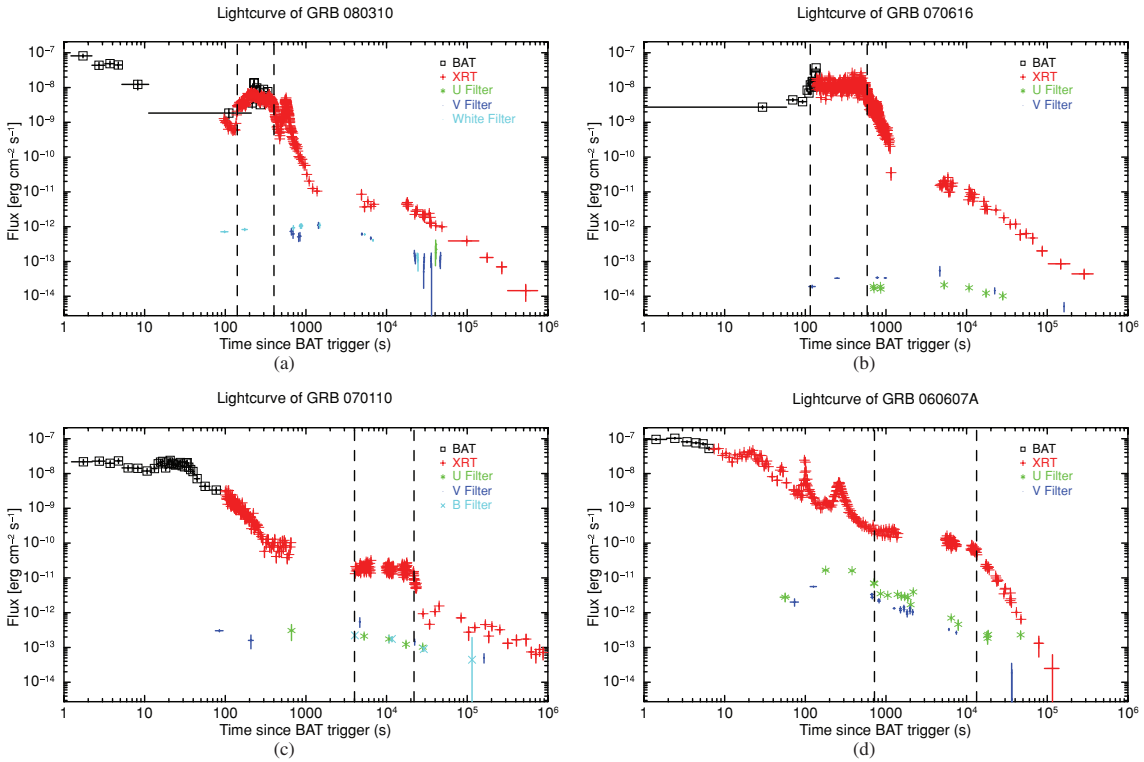

Figure 3. Combined BAT, XRT and UVOT light curves for the four GRBs with multiwavelength data during the internal plateau. The vertical dashed lines indicate the time interval over which the internal plateau dominates the emission. The optical data have been scaled down by a factor of 10 for panels (a) and (c).

with the two-component model. However, at late times the decay following the plateau is too steep for an afterglow and is consistent with $\alpha \sim 4$. This is unlikely to be explained by anything other than central engine activity and thus has been included in the internal plateau sample. As in GRB 070110, the internal plateau seen in GRB 060607A dominates the burst emission unusually late starting at about 900 s when (from Table 1) most of the other internal plateaus have ended.

GRB 060510B (also shown in Fig. 1) is very similar to GRB 070616. In both cases, the proposed internal plateau dominates the emission from the burst very early on.

GRB 060202 displays unusual emission attributed to an internal plateau between 325 and 766 s. The fluctuations during this plateau are unusually regular.

GRB 050904 has multiple flares at early and late times, but at about 230 s there is a period where the emission appears relatively constant followed by a steep decay, leading it to be included in the sample as a possible internal plateau.

To further investigate the nature of the internal plateau, we compared the X-ray data to optical/ultraviolet (UV) data from the UVOT. The GRBs within the sample with near-simultaneous optical/UV and X-ray light curves are shown in Fig. 3. While an early rise in the optical can be seen in some cases, the optical emission does not show the same behaviour as the X-ray. The internal plateau and following steep decay are significantly more prominent in X-rays. For example in GRB 070616, the optical is constant from before the plateau in the X-ray and until after the steep decline.

In Fig. 2, if the plateau seen in each of the X-ray light curves is of an external origin, then the X-ray and optical light curve should be related to each other in a manner consistent with the external shock model, i.e. the breaks should be achromatic. However, if the X-ray and optical emission components are not related to each other, for example a sharp decay in X-ray but no break in optical, this strongly suggests that the X-ray emission is not external or a jet-break but rather is of internal origin.

In Troja et al. (2007), for GRB 070110 four spectral energy distributions (SEDs) were examined during the initial decay, the beginning and the end of the plateau and during the shallow decay after the steep decline. These SEDs were constructed by extrapolating the X-ray spectrum to the lower energies. During the initial decay, the optical data are not consistent with the extrapolation of the X-ray spectrum to low energies. During the internal plateau, the optical and X-ray spectral distributions are also completely inconsistent with one another, implying different origins for the optical and X-ray photons.

For GRB 080310 and GRB 070616, the extrapolation of the X-ray spectrum is also inconsistent with the optical during the internal plateau (Beardmore et al., in preparation; Starling et al. 2008). Likewise, for GRB 060607A extrapolating the X-ray spectrum to the optical in a similar way to Troja et al. (2007) gives a poor fit to the optical (reduced χ^2 of 15.1). From this we conclude that during the internal plateau, the X-ray and optical emission have separate origins for the four GRBs for which we have multiwavelength data. Henceforth, we concentrate on the X-ray behaviour of our sample.

As the time at which the internal plateau ends differs markedly (cf. GRB 070110 and GRB 070616), it is possible that they have a different origin. Thus we further subdivide the sample into those GRBs in which the constant emission phase ends before or after 10 000 s. Those which end before 10 000 s are denoted as having early internal plateaus, whereas those ending after this time have late internal plateaus. In the next section, we compare the results for

these two groups to determine if their properties are consistent with being caused by the same physical process and whether that process is consistent with being due to a magnetar. Of the eight GRBs in the early internal plateau group, five have a redshift measurement as do both GRBs in the late plateau group. For the three GRBs with no redshift measurement, we adopt a redshift of 2.22, the mean redshift of *Swift* GRBs to determine the luminosity. Our conclusions are not sensitive to this choice.

4 THE MAGNETAR MODEL

In order to generate the intense magnetic fields required for a protomagnetar, a massive star's magnetic field must be increased as it collapses through magnetic flux conservation or efficient dynamo action (Dai & Lu 1998). This can be used to make a prediction for the initial period of the protomagnetar; every time the star collapses inwards by a factor of 2, the magnetic fields are increased by a factor of 4. To build up sufficient dynamo action on the surface, the star needs an initial rotation period of $\leq$10 ms (Usov 1992). Another method to predict the shortest rotation period is to use the breakup spin period for a neutron star, which is $\geq$0.96 ms (Lattimer & Prakash 2004). The initial rotation period of milliseconds is thought to differentiate between a protomagnetar and a neutron star. From a theoretical estimate, the limits set for the expected strong magnetic field are $B \geq 10^{15}$ G (Thompson 2007).

To place limits on the central object, we assume that the GRB jet is launched by the collapse of a massive star to a magnetar which survives for a short period of time before it collapses to a black hole (see Thompson 2007 for a review on the magnetar GRB central engine models). A transitory protomagnetar could cause the flux to remain roughly constant throughout the plateau until the protomagnetar had spun-down enough for the rotational energy to be insufficient to support the star. It would then collapse to form a black hole ceasing the plateau-like emission and causing the steep decay following the plateau. Flares during the plateau-like emission or the steep decline can arise from accretion on to the central object.

We use equations (2) and (3) (see Zhang & Mészáros 2001) to relate the continuous injection luminosity of the plateau, L, and the rest-frame time at which the plateau breaks down, τ, to the magnetar magnetic field and initial period:

$$L \simeq 10^{49} B_{\rm p,15}^2 P_{0,-3}^{-4} R_6^6 \ {\rm erg\ s^{-1}}, \quad (2)$$

$$\tau = 2.05 \times 10^3 I_{45} B_{\rm p,15}^{-2} P_{0,-3}^2 R_6^6 \ {\rm s}. \quad (3)$$

We use the GRB spectral shape and a k-correction (Bloom, Frail & Sari 2001) to convert the observed 0.3–10 keV flux to the rest-frame 1–1000 keV luminosity. $B_{\rm p}$ is the magnetic field strength at the poles where $B_{\rm p,15} = B_{\rm p}/10^{15}$ G, $P_{0,-3}$ is the initial rotation period in milliseconds, I_{45} is the moment of inertia in units of 10^{45} g cm^2 and R_6 is the stellar radius in units of 10^6 cm. If we use standard values for a neutron star (Stairs 2004) of mass $\sim$1.4 $M_\odot$ and $R_6 \sim 1$, then using equations (2) and (3) we can infer the central object's initial rotation period and magnetic field strength. The correlation between the derived period and the magnetic field is shown in Fig. 4.

In theory, there should be GRBs in the lower-right portion of Fig. 4 with a relatively long period and low dipolar field strength. From equation (2), a lower luminosity is expected for these GRBs, and hence it may be that the internal plateau is too faint to be observable. GRBs are unlikely to be present in the top-left as they would require extreme magnetic fields.

The derived periods are close to the submillisecond breakup limits for a neutron star, so it could be that most stars cannot support a temporary magnetar and collapse immediately to a black hole. If the initial rotation of the protomagnetar was violated by the breakup limit for a neutron star's period, it is unlikely that it could become stable enough to survive for the lengths of time given in Table 1. This results in a natural boundary on the left-hand side of Fig. 4. Thus only a small group of GRBs may produce an observable plateau, and this could explain the apparent correlation in Fig. 4.

The rotational energy reservoir of the magnetar given in Table 2 was calculated using equation (4) with $R_6 = 1$ and is consistent with the total power of the internal plateau ($E_{\rm iso,plat}$) as it should be

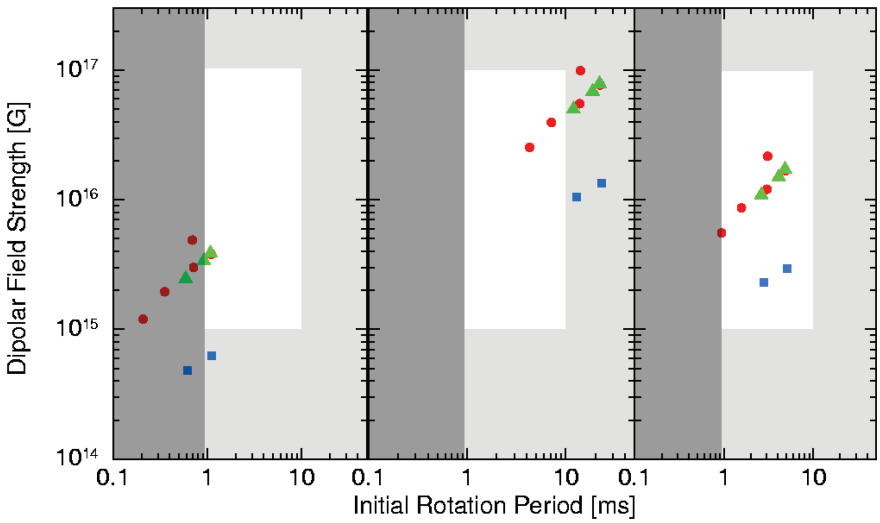

Figure 4. The initial period and magnetic field for each of the GRBs examined. In the left-hand panel, it was assumed that energy was released isotropically, whereas in the middle and right-hand panels it is beamed with an opening angle of 4° and 18°, respectively. GRBs with red filled circles have known redshifts and their internal plateaus occur during the prompt emission; GRBs shown by blue filled squares have known redshifts and their internal plateaus occur after the prompt emission; GRBs shown by green filled triangles have internal plateaus that occur during the prompt emission at unknown redshifts, and for which the redshift has been assumed to be equal to the median redshift of the *Swift* sample, meaning their parameters are more uncertain. The light grey shaded regions show limits based on the magnetic field and period limits discussed in the literature (see the text for details). The darker grey shaded region shows where a progenitor would be violating the breakup spin period of a neutron star.

Table 2. The different beamed energies found for the plateau for different opening angles compared to the energy of the actual GRB and the energy available in the rotational energy reservoir. All energies in the table are in erg; the opening angles used to find the beamed energy, respectively, are 4° and 18°. The $E_{\rm iso}$ values were derived from light curves with the 0.3–10 keV band.

GRB	Isotropic P_0 (ms)	Isotropic $B_{\rm p}$ ($\times 10^{16}$ G)	Beamed P_0 (ms)	Beamed $B_{\rm p}$ ($\times 10^{16}$ G)	$E_{\rm iso}$	$E_{\rm rot}$	$E_{\rm iso,plat}$	$E_{\gamma 1,{\rm plat}}$ ($\theta_j = 4$)	$E_{\gamma 2,{\rm plat}}$ ($\theta_j = 18$)
080310	0.7	0.3	13.8	5.5	2.91e+53[1]	3.90e+52	4.00e+52	9.75e+49	5.29e+51
071021	0.7	0.5	14.1	9.9	3.53e+53[2]	4.15e+52	4.25e+52	1.04e+50	8.45e+51
070721B	1.1	0.4	22.3	7.7	1.72e+53[3]	1.64e+52	1.69e+52	4.11e+49	1.27e+51
070616	0.6	0.2	12.0	5.0	2.47e+54[4]	5.74e+52	2.93e+53	7.13e+50	1.50e+52
070129	0.9	0.3	18.7	6.9	3.98e+53[5]	2.34e+52	1.07e+53	2.62e+50	5.51e+51
070110	1.1	0.06	23.2	1.3	7.08e+52[6]	1.61e+52	1.65e+52	4.02e+49	1.07e+51
060607A	0.6	0.04	12.4	1.0	2.13e+53[7]	5.35e+52	5.48e+52	1.34e+50	8.89e+51
060510B	0.2	0.1	4.2	2.5	1.09e+54[8]	4.64e+53	4.76e+53	1.16e+51	1.78e+52
060202	1.1	0.4	22.0	6.9	3.08e+53[9]	1.70e+53	8.33e+52	2.03e+50	4.27e+51
050904	0.4	0.2	7.1	4.0	2.51e+54[10]	1.61e+53	1.65e+53	4.01e+50	3.17e+52

References: [1]Tueller et al. (2008); [2]Barbier et al. (2007); [3]Palmer et al. (2007); [4]Sato & Barthelmy (2007); [5]Krimm et al. (2007); [6]Cummings et al. (2007); [7]Tueller et al. (2006); [8]Barthelmy et al. (2006); [9]Hullinger et al. (2006); [10]Sakamoto et al. (2005).

given the way magnetic field and initial period are calculated:

$$E_{\rm rot} = 2 \times 10^{52} M_{1.4} R_6^2 P_{0,-3}^{-2} \ {\rm erg}. \quad (4)$$

The plateau energy, $E_{\gamma,{\rm iso}}$, was calculated assuming that the radiation is emitted isotropically but it is almost certainly collimated by a relativistic wind flowing through a cavity produced by the elongation of a bubble of plasma and magnetic field (Bucciantini et al. 2007). This can be corrected for using

$$E_\gamma = f_{\rm b} \times E_{\gamma,{\rm iso}}, \ \text{where} \ f_{\rm b} = (1 - \cos\theta_j) = 0.5 \times \theta_j^2, \quad (5)$$

where θ_j is the opening angle of the beam. The maximum beaming angle ($\theta = 18°$) was estimated by assuming the fastest possible period as the breakup spin period of a neutron star. Taking this angle as the beaming angle for each GRB, the corresponding beaming-corrected energies are shown in Table 2 along with an example of the beaming-corrected energies derived using a beaming angle of 4° (Frail et al. 2001). A factor which affects the comparison of these energies is that the true initial rotation period is likely to be smaller than that derived from equation (4) (Thompson 2007), so $E_{\rm rot}$ could be larger.

The correlation between plateau luminosity and duration is shown in Fig. 5, which suggests that higher luminosity plateaus are generally of shorter duration. There are too few GRBs in the late internal plateau group to draw any firm conclusions. Their luminosities are lower, but not much lower than that of the early internal plateau group.

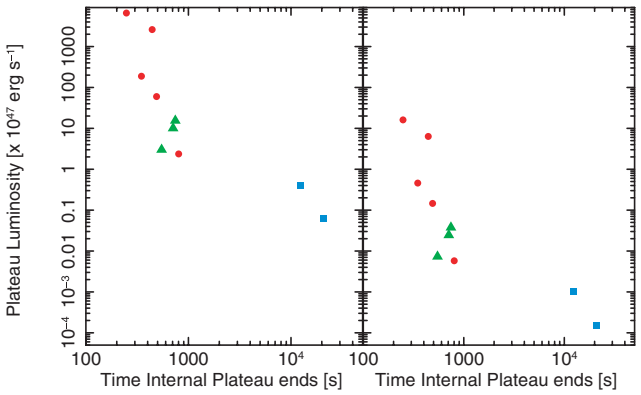

Figure 5. The relationship between the length of the internal plateau emission and its luminosity in the observer's frame, where it was assumed that energy was released isotropically in the left-hand panel and beamed with an opening angle of 4° in the right-hand panel. GRBs with red filled circles have known redshifts and their internal plateaus occur during the prompt emission, GRBs shown by blue filled squares have known redshifts and their internal plateaus occur after the prompt emission. The GRBs shown by green filled triangles have internal plateaus that occur during the prompt emission at unknown redshifts.

5 DISCUSSION

We have identified a small number of GRBs which display a period of time during which the X-ray emission shows a smooth plateau followed by a steep decline. The internal plateau is challenging to interpret using accretion models as it requires a constant power jet component with a roughly constant radiation efficiency. This possibility has been examined by Kumar, Narayan & Johnson (2008a), who suggest that the prompt emission of a GRB may be caused by the accretion of the outer regions of a stellar core and that the X-ray plateau could be caused by the fallback and accretion of the stellar envelope. This model has problems accounting for the steep declines seen after the plateau. Even assuming a sharp edge to the region being accreted, the steepest decline expected is $\alpha \sim 2.5$ (Kumar, Narayan & Johnson 2008b).

Here, we argue that a more natural explanation may come from the magnetar model which predicts a period of constant spin-down power. This model starts with the assumption that the neutron star accretor can power the GRB prompt emission which, while not certain, is feasible (Usov 1992; Thompson 1994; Bucciantini et al. 2007). Comparison of the luminosity and duration of the internal plateaus observed in our GRB sample with the dipolar spin-down law (Zhang & Mészáros 2001) implies upper limits to the magnetic field strengths close to the maximum allowed for such objects and initial spin periods also close to the maximum allowed to maintain neutron star structural integrity. The upper limits for the dipolar magnetic field of the magnetar are particularly strong if the emission is strongly beamed.

The largest magnetic fields implied for isotropic emission are consistent with field strengths of $\times 10^{16}$ G which can be generated in magnetars born with spin of a few milliseconds (Thompson & Duncan 1993; Duncan 1998). A giant flare from SGR 1806-20 on 2004 December 27 demonstrated that unless such flares are much rarer than the rate implied by detecting one, magnetars must possess a magnetic field strength of $\sim 10^{16}$ G or higher. Indeed values up to

$\sim 10^{17}$ G could not be ruled out (Stella et al. 2005). For the GRB sample in this paper, this could allow beaming factors corresponding to jet opening angles of 4°–10°, consistent with the values derived from Frail et al. (2001).

The number of GRBs that display internal plateau behaviour is very small. This perhaps is not surprising as we would expect them to only be detectable for quite a narrow combination of magnetic field strength and initial spin period. These rare features do provide limits on the magnetic fields surrounding the central engine around the GRB, and can help advance understanding of the mechanisms behind prompt emission.

ACKNOWLEDGMENTS

We gratefully acknowledge funding for *Swift* at the University of Leicester by the Science and Technology Facilities Council, in the USA by NASA and in Italy by contract ASI/INAF I/088/06/0. NL and RLCS also acknowledge funding by STFC via a studentship and PDRA, respectively. BZ and NL acknowledge funding by NASA grants NNG05GB67G and NNX08AN24G. We are also very grateful to our colleagues on the *Swift* project for their help and support, particularly Kim Page for providing the BAT and XRT light curves.

REFERENCES

Barbier L. et al., 2007, GCN 6966
Barthelmy S. et al., 2006, GCN 5107
Bloom J. S., Frail D. A., Sari R., 2001, ApJ, 121, 2879
Bucciantini N., Quataert E., Arons J., Metzger B. D., Thompson T. A., 2007, MNRAS, 380, 1541
Cummings J. R. et al., 2007, GCN 6007
Dai Z. G., Lu T., 1998, A&A, 333, L87
Duncan R. C., 1998, ApJ, 498, L45
Duncan R. C., Thompson C., 1992, ApJ, 392, L9
Evans P. A. et al., 2009, MNRAS, 397, 1177
Frail D. A. et al., 2001, ApJ, 562, 55
Hullinger D. et al., 2006, GCN 4635
Katz J. I., 1994, ApJ, 422, 248
Krimm H. et al., 2007, GCN 6058
Kumar P., Narayan R., Johnson J. L., 2008a, A&A, 388, 1729
Kumar P., Narayan R., Johnson J. L., 2008b, Sci, 321, 376
Lattimer J. M., Prakash M., 2004, Sci, 304, 536
Liang E., Zhang B., Zhang B., 2007, ApJ, 670, 565
Mészáros P., Rees M. J., 1997, ApJ, 476, 232
Nousek J. A. et al., 2006, ApJ, 642, 389
O'Brien P. T. et al., 2006, ApJ, 647, 1213
Palmer D. et al., 2007, GCN 6643
Rosswog S., Ramirez-Ruiz E., 2003, AIP Conf. Ser. Vol. 727, p. 361
Rees M. J., Mészáros P., 1994, ApJ, 430, L93
Sakamoto T. et al., 2005, GCN 3938
Sari R., Piran T., 1997, ApJ, 485, 270
Sari R., Piran T., Narayan R., 1998, ApJ, 497, L17
Sato G., Barthelmy S., 2007, GCN 6551
Stairs I. H., 2004, Sci, 304, 547
Starling R. L. C. et al., 2008, MNRAS, 384, 504
Stella L. et al., 2005, ApJ, 634, L165
Thompson C., 1994, MNRAS, 270, 480
Thompson C., Duncan R. C., 1993, ApJ, 408, 194
Thompson T. A., 2007, Rev. Mex. Astron. Astrofis. Conf. Ser., 27, 80
Troja E. et al., 2007, ApJ, 665, 599
Tueller J. et al., 2006, GCN 5242
Tueller J. et al., 2008, GCN 7402
Usov V. V., 1992, Nat, 357, 472
Willingale R. et al., 2007, ApJ, 662, 1093
Zhang B., Mészáros P., 2001, ApJ, 552, L35
Zhang B. et al., 2006, ApJ, 642, 354

This paper has been typeset from a TEX/LATEX file prepared by the author.